ORIGINAL PAPER

Brownian dynamics study of flux ratios in sodium channels

Taira Vora · Ben Corry · Shin-Ho Chung

Abstract Measurements of unidirectional fluxes in ion channels provide one of the experimental methods for studying the steps involved in ion permeation in biological pores. Conventionally, the number of ions in the pore is inferred by fitting the ratio of inward and outward currents to an exponential function with an adjustable parameter known as the flux ratio exponent. Here we investigate the relationship between the number of ions in the pore and the flux ratio exponent in a model sodium channel under a range of conditions. Brownian dynamics simulations enable us to count the precise number of ions in the channel and at the same time measure the currents flowing across the pore in both directions. We show here that the values of the flux ratio exponent n' ranges between 1 and 3 and is highly dependent on the ionic concentrations in which measurements are made. This is a consequence of the fact that both inward and outward currents are susceptible to saturation with increasing concentration. These results indicate that measurements of the flux ratio exponent cannot be directly related to the number of ions in the pore and that interpretation of such experimental measurements requires careful consideration of the conditions in which the study is made.

Keywords Ion channel · Electrophysiology · Flux ratio · Sodium channel · Brownian dynamics · Permeation

T. Vora · S.-H. Chung
Research School of Biological Sciences, The Australian National University, Canberra, Australia

B. Corry (✉)
School of Biomedical, Biomolecular and Chemical Sciences,
The University of Western Australia,
Crawley, WA 6009, Australia
e-mail: ben.corry@uwa.edu.au

Introduction

Understanding the steps involved in ion permeation through biological ion channels has been one of the major goals of ion channel research. Using experimental techniques to reveal how individual ions move through single ion channels experimentally is a difficult task. High resolution x-ray diffraction data has enabled the average number and positions of ions to be seen in a static picture in one case (Morais-Cabral et al. 2001), but such data has remained elusive for most channel forming proteins. Recent advances in simulation techniques have allowed some of these steps to be probed at a molecular level, but accurate simulations generally require high resolution experimental structural data as a starting point and validation of the simulation ideally requires experimental data relating to the behaviour of ions in the pore.

Measurements of the unidirectional fluxes of ions through channels has been one of the only techniques available for determining how ions interact within pores, as their ratio is related to the number of ions in the pore (See, for example, Begenisich and Busath 1981; Rakowski et al. 2007). The nature of this relationship, however, is often misunderstood. If ion permeation is to be studied experimentally, it is imperative that the implications of unidirectional flux measurements be clarified. Here we aim to do this using a simulation technique that allows us to simultaneously measure the current of ions passing through a model sodium channel as well the number of ions contained within it.

Since the middle of the last century, attempts have been made to infer the mechanisms underlying ion permeation through individual ionic pores from careful measurements of the inward and outward currents flowing across cell membranes. Initial descriptions assumed that ions moved

through these pores independently, not interacting with other ions along the way (Ussing 1949). Under these conditions the ratio between efflux (I_{out}) and influx (I_{in}) across the membrane is given by the expression (Ussing 1949),

$$\frac{I_{out}}{I_{in}} = \frac{[S]_i}{[S]_o} \exp(V_m F/RT) \qquad (1)$$

where $[S]_i$ and $[S]_o$ are the internal and external ion activities of ion type S and V_m is the membrane potential. The terms R, T and F have their usual thermodynamic meanings.

It soon became apparent, however, that the notion of independence did not hold for most pores. The ratio of inward and outward potassium currents through giant squid axon, for example, were shown to deviate from that expected for independent ion movement. This ratio changed 2400-fold as the electrochemical potential $V_m - V_K$ (V_K is potassium equilibrium potential) was altered between -50 and $+30$ mV (Hodgkin and Keynes 1955). Hodgkin and Keynes (1955) suggested that in long pores, where more than one ion was present, ions could interact with one another and thus the potassium movements were not independent. This is most easily visualised using single file models of pores in which ions move between sites in which they linger (usually termed 'binding sites') in a correlated fashion such that an ion must leave one site in order for another ion to replace it. Such coupled transport is now believed to be a common mechanism of ion permeation in potassium channels and many other pores, and has been described in detail by a number of kinetic models that simulate the sequential hopping of ions between sites (Heckmann 1965a, b, 1968, 1972; Hille and Schwarz 1978). This knock-on movement of ions is also apparent in physical models of conduction in potassium channels (Chung et al. 2002; Berneche and Roux 2001).

Hodgkin and Keynes (1955) showed that their data would fit the above equation for the rates of efflux to influx only if it were raised to a power n', called the flux ratio exponent,

$$\frac{I_{out}}{I_{in}} = \exp(n'[V_m - V_S]F/RT) \qquad (2)$$

Measured values of n' for the potassium channels range between 1.5 and 3.3 depending on the membrane potential and internal potassium concentrations (Begenisich and DeWeer 1980).

Since then, the presence of a flux ratio exponent, $n' > 1$ is taken as a signature of a multi-ion pore. The value of the flux ratio is related to the number of binding sites, or perhaps more accurately, the number of ions in the pore. Measurements for potassium channels, therefore indicate that there may be as many as three binding sites in the

channel, an interpretation that has been validated by X-ray crystal structures indicating the presence of up to three ions in the channel at one time (Doyle et al. 1998; Zhou et al. 2001).

A difficulty in the interpretation of n', however, is that its value can vary depending on the conditions in which it is measured. Using the rate models of single file diffusion it can be shown that the value of the flux ratio exponent of the pore can vary from anywhere between 1 and the number of binding sites, n (Heckmann 1972; Hille and Schwarz 1978). A given measurement of the flux ratio exponent cannot, therefore, be directly related to the number of binding sites or ions involved in permeation, but rather it can only yield a minimum value for the conditions studied. Despite this, it is not uncommon to see measurements of a flux ratio exponent of one taken to imply a single ion pore (Begenisich and Busath 1981; Rakowski et al. 2002, 2007).

It is worth adding a clarifying comment about the nature of knock-on ion diffusion in single file pores. The classic picture envisioned by Hodgkin and Keynes (1955) involved all binding sites in the pore being permanently occupied, a situation that leads to a high flux ratio exponent $n' = n + 1$. Heckmann (1972), in contrast pictured the situation in which a binding site must become empty before an ion can move into it, which in general will yield lower values of n'. The determination of crystal structures and physical models of ion conduction suggests that both these pictures capture some element of reality. The selectivity filter of KcsA, for example, contains four binding sites, yet is expected to contain only two ions even at high concentrations (Doyle et al. 1998; Zhou et al. 2001). But, the long range ion-ion repulsion that prevents ions from packing in more densely to the pore can also mediate knock-on conduction across empty sites and yield a similar knock-on phenomenon that includes the motion of vacancies. Vacancy inclusive knock-on conduction yields a range of possible flux ratio exponents as for Heckmann's models.

The interpretation of the flux ratio exponent is particularly interesting in the case of sodium channels. Begenisich and Busath calculated the flux ratio exponent for transport through sodium channels in giant squid axon at a number of internal sodium concentrations and membrane potentials and found it to be $n' \sim 1$ (Begenisich and Busath 1981). They suspected from earlier measurements (Begenisich and Cahalan 1980) that sodium channels act like multi-ion pores but thought that the low value of the flux ratio exponent might mean that although there could be two binding sites in the channel that they are rarely filled simultaneously. More recent measurements of Na^+ flux have also found $n' \sim 1$ and implied this to mean single ion occupancy (Rakowski et al. 2002).

This result is intriguing as it appears incompatible with sodium channels utilising multi-ion permeation taking place via a knock-on mechanism as believed to occur in potassium channels. There are, however, reasons for believing that sodium channels will hold multiple ions as discussed previously (Vora et al. 2005). Firstly, there are a large number of negatively charged residues believed to surround the selectivity filter (with a net charge of −5 if all fully charged) that are likely to attract multiple ions into the pore. It is difficult to imagine a situation in which they are either protonated or orientated in such a way that could also explain the effect of mutations on these residues if they were not imparting large electrostatic forces on permeant ions (Heinemann et al. 1992; Schlief et al. 1996; Sun et al. 1997). Secondly, the fact that the channel is known to strongly bind divalent Ca^{2+} ions (French et al. 1994) also implies that it would have a good chance of binding at least two monovalent ions. Finally, simulations on model sodium channels suggest multiple occupancy (Vora et al. 2005).

The apparent paradox between flux ratios suggesting single ion pores and other data implying multiple occupancy needs to be resolved. We make use of Brownian dynamics simulations to better understand the steps involved in permeation and also the relationship between the flux ratio exponent and the number of ions in the channel. This technique allows for the flux passing through the pore as well as the number of ions, their locations and the steps involved in permeation to be directly determined from the same simulation. To this end we use a model of sodium channels that has previously been shown to accurately reproduce the experimental current–voltage curves, current-concentration curves, and block of monovalent ion by divalent ions (Vora et al. 2005). Although we hope that this model is relatively accurate, in the current situation we are most interested in directly comparing how the measurable flux ratio exponent relates to the number of ions residing in the pore during the same simulations. This allows us to examine the general behaviour of the flux ratio exponent in differing conditions, rather than necessarily describing the reality of sodium channel permeation.

Methods

Channel model

The sodium channel model used in this work has been described previously (Vora et al. 2005). As pictured in Fig. 1 the shape of the pore is loosely based on the structure of the KcsA potassium channel, with a minimum diameter of 4.4 Å determined from the size of the largest permeant cation (Hille 1971). Two rings of charged residues, EEDD and DEKA, are included to represent the residues known to have an important role in ion permeation selectivity. Best agreement with experimental data is obtained assuming that approximately two of these residues are protonated such the outer ring has a net charge of -3.8×10^{-19} C and the inner ring has a charge of -1.0×10^{-19} C. For complete details on the construction and testing of this model we refer the reader to Vora et al. (2005).

Brownian dynamics simulations

Brownian dynamics (BD) simulations have been successfully applied to study the motion and current of ions through potassium, calcium, sodium and other channels (Corry et al. 2001; Chung et al. 2002; Vora et al. 2005) and we refer the reader to these earlier publications for more details. The motion of individual ions is traced explicitly, but the water and protein atoms are treated as continuous dielectric media that exert random and frictional forces on the ions (Li et al. 1998; Chung et al. 2002). Unlike in molecular dynamics simulations, the protein forming the pore in BD is assumed to be rigid. It has been postulated that fluctuations of the fully or partially charged moieties lining the pore may play a significant role in the mechanism of ion selectivity (Allen et al. 2004). We devised the method of incorporating the motion of charged atoms in BD and examined the dynamics of ion permeation across the KcsA potassium channel using the rigid and flexible carbonyl groups lining the selectivity filter. The number of resident ions in the channel and the locations of the binding sites remain unchanged under these two conditions. The movement of the carbonyl group had only a small influence on the computed current (Chung and Corry 2007). In addition, as the aim of the present study is to
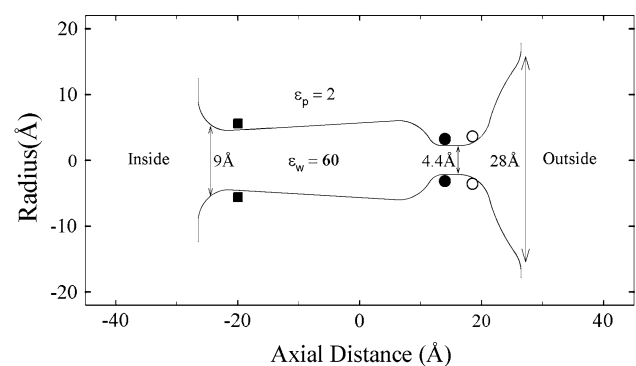

Fig. 1 Sodium channel model. The sodium channel model is generated by rotating each curve by 180°. The points marked by open and closed circles around the selectivity filter represent the position of the two rings of EEDD and DEKA residues respectively. The squares correspond to the negative dipoles (each with charge -0.6×10^{-19} C) at the end of the protein

calculate unidirectional fluxes in a model in which we can simultaneously count ions in the pore rather than attempting to present a detailed model of sodium channels, we use a rigid protein here.

A number of Na^+ and Cl^- ions are placed in cylindrical reservoirs of radius 30 Å at each end of the channel that mimic the intra- and extra-cellular solution, and the height of the cylinder is adjusted to bring the solution to the desired concentration. A more detailed explanation of the reservoirs and a comparison with other methods of maintaining ion concentrations has been published previously (Corry et al. 2002). The motion of these ions under the influence of electric and random forces is then traced using the Langevin equation. The total force acting on each and every ion in the assembly is calculated and then new positions are determined for the ions a short time later. Electrostatic forces are calculated by assigning dielectric constants of 2 to the protein and 60 to the water in the channel and solving Poisson's equation using an iterative method (Hoyles et al. 1998). The current passing in each direction is determined directly from the number of ions passing through the channel.

Calculation of the flux ratio exponent

The flux ratio exponent can be calculated from the expression

$$n' = \frac{RT}{(V_m - V_{Na})F} \ln \frac{I_{out}}{I_{in}} \quad (3)$$

where V_{Na} is Nernst potential for sodium given by,

$$V_{Na} = \frac{RT}{F} \ln \frac{[Na]_o}{[Na]_i} \quad (4)$$

Here $[Na]_o$ and $[Na]_i$ are the external and internal activities for sodium, respectively. If we calculate the flux ratio exponent for sodium channels at a membrane potential of $V_m = 0$, and substitute the value of V_{Na} from Eq. 4 into Eq. 3 we obtain the simpler situation,

$$n' = \frac{\ln\left(\frac{I_{in}}{I_{out}}\right)}{\ln\left(\frac{[Na]_o}{[Na]_i}\right)} \quad (5)$$

To examine how the flux ratio exponent depends on the concentration of ions, we calculated its value for a number of different internal and external concentrations. It is of interest to examine whether n' is dependent on the magnitude of the ion concentrations or just their ratio. To this end, we altered the concentration on either side of the pore, while maintaining the same ratio $[Na]_o/[Na]_i$ and calculated the value of the flux ratio.

We performed BD simulations with three different concentration ratios; these were $[Na]_o/[Na]_i = 1.25, 2.49$

and 3.36. This ratio was calculated by dividing the external and internal reservoirs into 8 separate bins, and calculating the average concentration. The Nernst potential for each of the concentration ratios was $V_{Na} = 5.7, 23.4$ and 31.0 mV, respectively. All simulations for the sodium channel model were performed at $V_m = 0$ mV apart from an initial simulation at −70 mV used as a control run to ascertain the location of the ions within the channel.

Once the simulations were performed at $V_m = 0$ mV, the inward and outward currents, I_{in} and I_{out} are calculated by counting the ions that cross the channel in each direction. All error bars we calculated by propagating the error in the current in each situation through the calculation of the flux ratio on n' and have length of twice the standard error.

Results

Before calculating flux ratio exponents, it is worth examining the dynamics of ions under symmetric concentrations and a membrane potential to see the steps involved in ion permeation. In Fig. 2b we plot a histogram indicating where ions dwell within the pore under an applied potential of −70 mV driving Na^+ into the cell. It is apparent that multiple ions occupy the charged narrow region of the pore. There are on average around 2.2 ions in this region. The steps involved in ion conduction are shown in Fig. 2a. Two ions are always found within the channel due to the electrostatic attraction of the charged residues. The entrance of a third ion is required to dislodge one of the ions, sending it across the centre of the channel in a knock-on mechanism. The rate of entrance of the third ion is likely to be concentration dependent, however, the rate of channel crossing by the left hand ion once the third ion enters on the right is not. This means that as the concentration of ions is increased, the current eventually saturates, as shown under symmetrical concentrations in Fig. 2c. The second step in conduction (t_2) therefore becomes the rate limiting step. In this channel model, conduction is clearly a multi-ion process. In Fig. 2c, the experimental measurements (filled circles) obtained by Schild et al. (1991) are superimposed on the simulated data (open circles).

Next we calculated the inward to outward flux ratio in BD simulations with no applied potential. To do this we varied the internal and external activities, while maintaining the ratio $[Na]_o/[Na]_i$ constant. This was done for three different activity ratios as plotted in Fig. 3.

If we were to assume that the value of n' is unchanged by sodium concentration, then we would expect to obtain a single I_{in}/I_{out} value in each of the three plots within Fig. 3. Furthermore, in a single ion channel, or in a situation where n' had a constant value of 1, using constant internal to
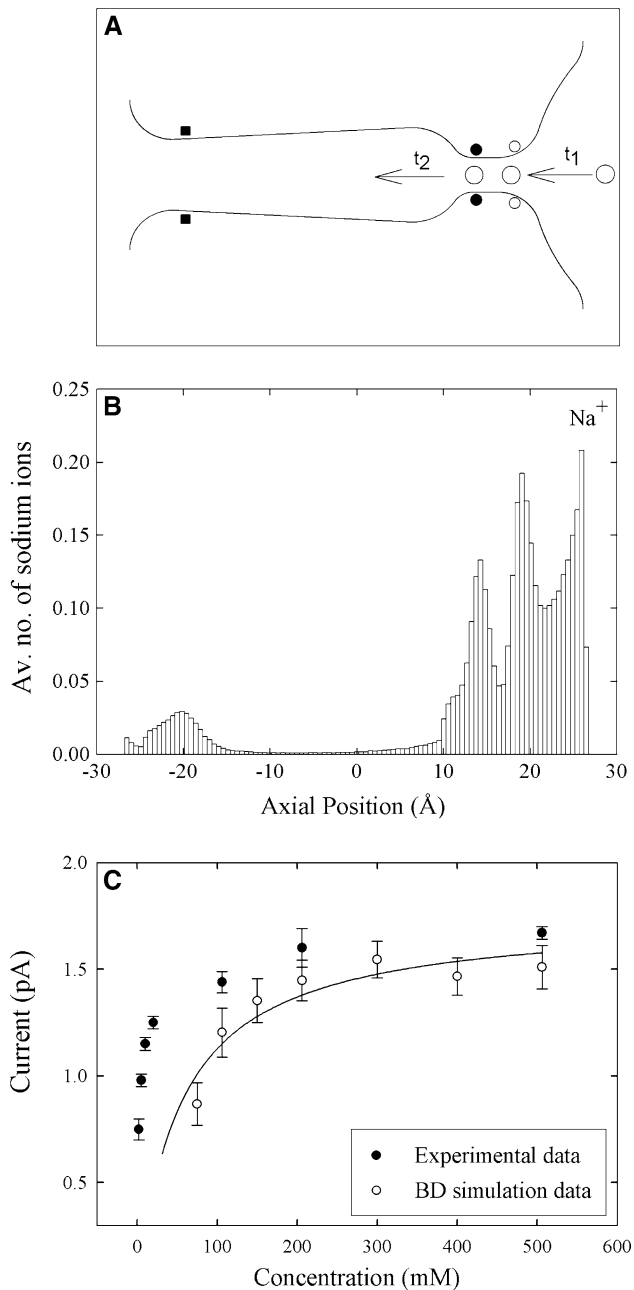
Fig. 2 Dynamics of ion permeation across the sodium channel under symmetric 200 mM NaCl and an applied potential of −70 mV. **a** The steps involved in multi-ion permeation across the pore is schematically illustrated. The time it takes for a conduction event to occur is composed of two parts: the time it takes for an ion to enter the pore, t_1, which is partly dependent on ionic concentrations, and the time it takes an ion bound to the internal binding site to exit the pore, t_2, which is independent of ionic concentrations. **b** Histogram showing the locations where ions preferentially dwell inside the pore. **c** The current-concentration curves obtained from BD simulations (*open circles*) and experimental measurements (*filled circles*) show that the currents increases rapidly with increasing ionic concentrations and then saturate. The experimental measurements are obtained by Schild et al. (1991)

external activity ratios, we would expect to see a constant flux ratio of 1.25, 2.5 and 3.36 for each of the three plots, respectively (Eq. 5). Clearly neither of these situations hold. As suggested in the rate models of unidirectional fluxes, the flux ratio in multi ion channels will vary with the ion concentration.

It can be clearly seen why the flux ratio exponent has such an enormous dependence on the surrounding ion concentrations by reconsidering Fig. 2c. Just as the net current passing through the channel saturates at large concentrations, the same can be expected of the unidirectional fluxes. Although the same activity ratio is used within each of the plots in Fig. 3, at the right hand end the outside concentration is above the value at which the ion current saturates, while the inside concentration is below this. Thus we can expect the ratio of inward to outward currents to drop.

Although the error bars are much larger, the trend of decreasing n' value with increasing concentration is also observed in a plot of the flux ratio exponent shown in Fig. 4. It is difficult to reduce the error bars in these plots due to the logarithmic function involved in calculating n'. However, the key result is clear, the value of the flux ratio exponent can be expected to change with ion concentration.

We also note that the number of ions inside the channel does not change significantly with changing concentration. With a fixed internal concentration of 77 mM the number of ions in the pore is 2.56 when the external concentration is 254 mM and 2.30 when it is 98 mM. The location of the ions is almost identical to that seen in Fig. 2a with only a marginally higher concentration in the external vestibule at high external concentration than at a low concentration. This suggests that the mechanism for permeation in the sodium channel remains unchanged despite varying external concentration: the channel holds two ions in the selectivity filter and outer vestibule and a third ion is required to enter for conduction to take place. Despite this, the value of the flux ratio exponent is significantly different, $n' = 1.44$ at the higher external concentration and $n' = 2.61$ at the lower one. Clearly, the value of the flux ratio exponent cannot be directly related to the number of ions in the pore unless the conditions in which the measurement are made are taken into account.

Can the fact that the current saturates with increasing concentration be built in to the formulation of the flux ratio exponent? Heckmann (1972) as well as Hille and Schwarz (1978) explain that $n' = n$ only under very specific conditions. This happens only when the rate at which ions jump between binding sites within the pore is greater than the rate at which they enter the pore, which is again much
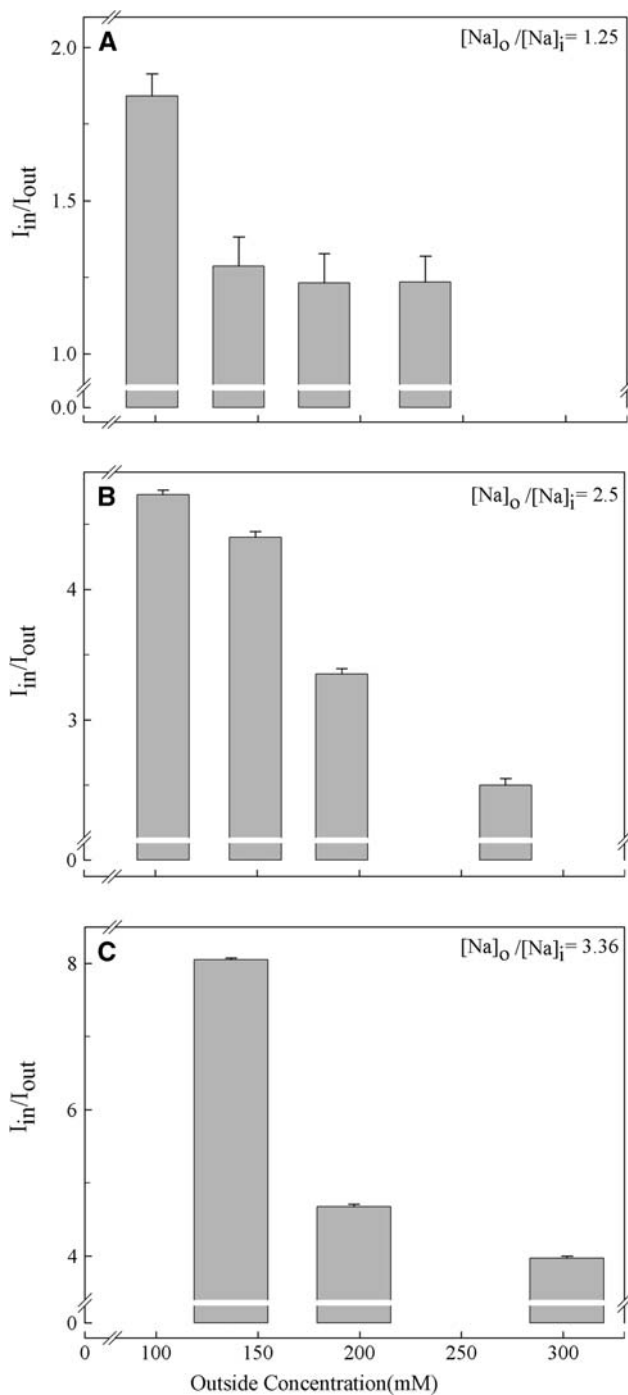
Fig. 3 The ratios of the inward and outward currents. The measured ratios are plotted against the external concentration for four different concentration ratios $[Na]_o/[Na]_i$: 1.25 (**a**), 2.5 (**b**) and 3.36 (**c**)

Fig. 4 Flux ratio exponents calculated from the data shown in Fig. 3, using Eq. (5)

greater than the rate at which they leave the pore. This represents the situation of low outside concentrations, when there are few ions around the entrance of the channel limiting the entry rate.

Having examined the value of the flux ratio exponent in this channel model, it is interesting to see how these results
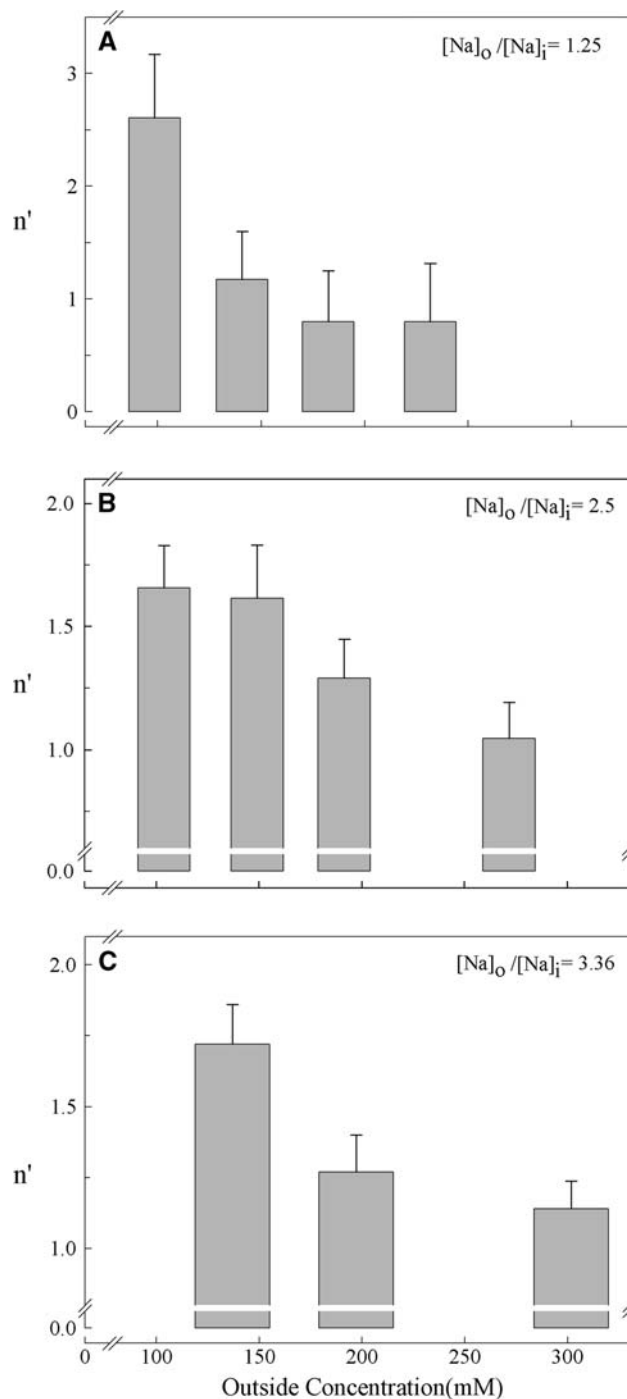
compare with experimental measurements made in squid giant axon. In the studies of Begenisich and Busath (1981) external sodium concentrations of 440 mM and internal concentrations of 50–200 mM were used. More recently, similar measurements used a concentration of 425 mM (Rakowski et al. 2002). Both experiments found a flux ratio exponent close to unity. An inspection of the

current-concentration curve either from our simulation (Fig. 2c) or from experimental measurements (French et al. 1994; Worely III et al. 1992; Schild and Moczydlowski 1994), however, indicates that at these concentrations, the inward current passing through the channel is likely to have saturated. Although these measurements were made under an applied potential, a comparison with our results suggest that it is entirely possible that at these concentrations, a low value of the flux ratio exponent is likely regardless of how many ions are involved in the permeation process. This result serves as a reminder that a measured flux ratio exponent of 1 does not necessarily imply a single ion conduction mechanism. It is also notable that the larger concentration for half saturation of typical potassium channels, as well as lower ion concentration used in the the classic measurements of flux ratios in potassium channels carried out by Hodgkin and Keynes (1955) and Begenisich and De Weer (1980) in combination with a higher binding affinity in potassium channels may have assisted in the experimental conditions yielding higher values of the flux ratio exponent.

Concluding remarks

Brownian dynamics simulations can explicitly model the motion of individual ions at the same time as predicting channel currents and is therefore an excellent tool to ascertain the relationships between the flux ratio, number of ions in the channel and experimental conditions. It is clear that the flux ratio exponent is highly dependent on the concentrations under which it is calculated. Caution must be applied, therefore, when interpreting values of the flux ratio exponent determined under high internal or external concentrations as one or more unidirectional fluxes may have saturated.

References

Allen TW, Andersen OS, Roux B (2004) On the importance of atomic fluctuations, protein flexibility, and solvent in ion permeation. J Gen Physiol 124:679–690

Begenisich T, Cahalan MD (1980) Sodium channel permeation in squid axons II: non-independence and current voltage relations. J Physiol 307:243–257

Begenisich T, DeWeer P (1980) Potassium flux ratio in voltage clamped squid giant axons. J Gen Physiol 76:83–98

Begenisich T, Busath D (1981) Sodium flux ratio in voltage clamped squid giant axons. J Gen Physiol 77:489–502

Berneche S, Roux B (2001) Energetics of ion conduction through the K+ channel. Nature 414:73–77

Chung SH, Corry B (2007) Conduction properties of KcsA measured using Brownian dynamics with flexible carbonyl groups in the selectivity filter. Biophys J 93:44–53

Chung SH, Allen TW, Kuyucak S (2002) Conducting-state properties of the KcsA potassium channel from molecular and Brownian dynamics simulations. Biophys J 82:628–645

Corry B, Allen TW, Kuyucak S, Chung SH (2001) Mechanisms of permeation and selectivity in calcium channels. Biophys J 80:195–214

Corry B, Hoyles M, Allen TW, Walker M, Kuyucak S, Chung SH (2002) Reservoir boundaries in Brownian dynamics simulations of ion channels. Biophys J 82:1975–1984

Doyle DA, Cabral JM, Pfuetzner RA, Kuo A, Gulbis JM, Cohen SL, Chait BT, MacKinnon R (1998) The structure of the potassium channel: molecular basis of K$^+$ conduction and selectivity. Science 280:69–77

French RJ, Worley III JF, Wonderlin WF, Kularatna AS, Krueger BK (1994) Ion permeation, divalent ion block, and chemical modification of single sodium channels. J Gen Physiol 103:447–470

Heckmann K (1965a) Zur Theorie der 'single file'-diffusion. part I. Z Phys Chem 44:184–203

Heckmann K (1965b) Zur Theorie der 'single file'-diffusion. part II. Z Phys Chem 46:1–25

Heckmann K (1968) Zur Theorie der 'single file'-diffusion. part III Sigmoide Konzentrationsabhängigkeit unidirectionaler Flüsse bei 'single file' diffusion. Z Phys Chem 58:201–209

Heckmann K (1972) Single file diffusion. Biomembranes 3:127–153

Heinemann SH, Terlan H, Stühmer W, Imoto K, Numa S (1992) Calcium channel characteristics conferred on the sodium channel by single mutations. Nature 356:441–443

Hille B (1971) The permeability of the sodium channel to organic cations. J Gen Physiol 58:599–619

Hille B, Schwarz W (1978) Potassium channels as multi-ion single-file pores. J Gen Physiol 72:409–442

Hodgkin AL, Keynes RD (1955) The potassium permeability of a giant nerve fibre. J Physiol 128:61–88

Hoyles M, Kuyucak S, Chung SH (1998) Solutions of Poisson's equation in channel-like geometries. Comp Phys Commun 115:45–68

Li SC, Hoyles M, Kuyucak S, Chung SH (1998) Brownian dynamics study of ion transport in the vestibule of membrane channels. Biophys J 74:37–47

Morais-Cabral JH, Zhou Y, MacKinnon R (2001) Energetic optimization of ion conduction rate by the K$^+$ selectivity filter. Nature 414:37–42

Rakowski RF, Gadsby DC, De Weer P (2002) Single ion occupancy and steady-state gating of Na channels in squid giant axon. J Gen Physiol 119:235–250

Rakowski RF, Artigas P, Palma F, Holmgren M, De Weer P, Gadsby DC (2007) Sodium flux ratio in Na/K pump-channels opened by palytoxin. J Gen Physiol 130:41–54

Schild L, Ravindran A, Moczydlowski E (1991) Zn^{2+}-induced subconductance events in cardiac Na$^+$ channels prolonged by batrachotoxin. J Gen Physiol 97:117–142

Schild L, Moczydlowski E (1994) Permeation of Na$^+$ through open and Zn^{2+}—occupied conductance states of cardiac sodium channels modified by batrachotoxin: exploring ion-ion interactions in a multi-ion channel. Biophys. J 66:654–666

Schlief T, Schönherr R, Imoto K, Heinemann SH (1996) Pore properties of rat brain II: sodium channels mutated in the selectivity filter. Eur Biophys J 25:75–91

Sun YM, Favre I, Schild L, Moczydlowski E (1997) On the structural basis for size selective permeation of organic cations through the

voltage gated sodium channel—effect of alanine mutations at the DEKA locus on selectivity, inhibition by Ca^{2+} and H^+, and molecular sieving. J Gen Physiol 110:693–715

Ussing HH (1949) The distinction by means of tracers between active transport and diffusion. Acta Physiol Scand 19:43–56

Vora T, Corry B, Chung SH (2005) A model of sodium channels. Biochim Biophys Acta 1668:106–116

Worely III JF, French RJ, Pailthorpe BA, Krueger BK (1992) Lipid surface charge does not influence conductance or calcium block of single sodium channels in planar bilayers. Biophys J 61:1353–1363

Zhou Y, Morais-Cabral JH, Kaufman A, MacKinnon R (2001) Chemistry of ion coordination and hydration revealed by a K+ channel-fab complex at 2.0 Å resolution. Nature 414:43–48